Enhanced Mechanical and Cytocompatibility Properties of Novel 3D Printed Osteochondral Scaffolds

B. Holmes*, L.G. Zhang* **

*School of Engineering and Applied Science, The George Washington University, Washington DC 20052, USA bbh2c@gwmail.gwu.edu ** Department of Mechanical and Aerospace Engineering, Department of Medicine, The George Washington University, Washington DC 20052, USA lgzhang@gwu.edu

ABSTRACT

As modern medicine advances, various methodologies are being explored and developed in order to treat various severe osteochondral defects in joints. However, it is still very challenging to cure the osteochondral defects due to its poor inherent regenerative capacity, complex stratified architecture and disparate biomechanical properties. The objective of the current work is to create novel 3D printed osteochondral scaffolds with both excellent interfacial mechanical properties and biocompatibility for facilitating human bone marrow mesenchymal stem cell (MSC) growth and chondrogenic differentiation. For this purpose, we designed and 3D printed a series of innovative bi-phasic 3D models which mimic the osteochondral region of articulate joints. In order to improve their biocompatibility, the scaffolds' surfaces were further modified with acetylated collagen (one of the main components in osteochondral tissue). MSC proliferation result demonstrated that incorporation of a collagen coating, along with biomimetically designed micro-features, can greatly enhance MSC growth after 5 days in vitro. Two weeks chondrogenic differentiation results showed that our novel scaffolds (dubbed "key" scaffolds), both with and without surface collagen modification, displayed enhanced chondrogenesis (i.e. glycosaminoglycan (GAG), collagen type II deposition and total protein content).

Keywords: Osteochondral, 3D printing, stem cell, tissue engineering, scaffold.

1 MATERIALS AND METHODS

1.1 3D osteochondral scaffold design and fabrication

All 3D osteochondral scaffolds were fabricated using a PrinterBot 3D printing system modified with a 347 µm diameter nozzle, and a spool of 1.75 mm diameter biocompatible Poly lactic acid (PLA) polymer. Our 3D printer consists of a heated printing bed (heated to 60ºC), a heated printing tool (heated headset to 185 ºC and extrusion motor) capable of 3D axial movement and a computer/controller using the Pronterface control software package. A series of CAD drawings converted to Sterelithography (stl) format (to be described next) were used in conjunction with Slic3r stl slicing software and the 3D printer to create predesigned 3D structures. The printing tool draws a PLA filament and forces it through a heated extruder nozzle, which melts and deposits polymer on the printing surface in a thin layer. The machine then prints multiple thin layers on top of the previously deposited layers to create various designed, fully solid 3D osteochondral constructs.

Moreover, we applied a collagen type I coating on one osteochondral scaffold (i.e., bi-phasic key osteochondral scaffold with small pores, expected to have optimized properties for our study) to further improve their cytocompatibility. A protocol for chemically functionalized attachment known as acetylation [[2]] was used. Briefly, the scaffolds were immersed in an ethylenediamine/n-propanol (1:9 ratio) solution at 60 ºC for 5 min. They were then extensively washed with deionized water and dried at 35 ºC. The aminolysed scaffolds were then immersed in a 1% gluteraldehyde solution at room temperature for 3 h to transfer the NH2 groups into CHO groups. After washing extensively, the scaffolds were immersed in 0.1% acetylated collagen at 4 ºC for 24 h. The process itself yields a series of layered chemical attachments, finally resulting in a collagen coating.

1.2 Mechanical testing, modeling and scaffold imaging

All mechanical testing including compressive and shear testing was conducted using a uniaxial testing system (ATS systems). For compression testing, a flat 2 cm diameter platen was attached to a 500 N load cell. The platen was then advanced into the scaffolds, oriented uniaxially with the bone layer on the bottom and the cartilage layer interacting with the platen, at a 0.02 cm/min strain rate. Data was taken using LabView, and then analyzed in Microsoft Excel. Load and displacement were used to plot the stress / strain curves and then Young's modulus was calculated from the linear elastic region. For shear testing, the same setup and conditions were used, with the exception of the platen being replaced with a 5º wedge (from centerline, 10º total) and the scaffold rotated 90º. The interface between the bone and cartilage layers was aligned parallel to the wedge, and the wedge was advanced into the interface line for bi-phasic and key scaffolds. For homogeneous models, the wedge was advanced into the scaffold at half of the scaffolds' height, which is consistent to the dimensions and orientations of the other two models.

Force was plotted against displacement and the area under the curve was taken to provide the shear fracture energy in N/mm2.

Based on the obtained experimental data, a computational model was composed to estimate and correlate the properties of various mciro structures with different porosities. In addition, a Zeiss SigmaVP Scanning Electron Microscope (SEM) was used to image the surfaces of acetylated collagen constructs and controls (uncoated scaffolds). Scaffolds were coated with an approximately 4~8 nm of gold nanoparticles and then isolated on carbon tape dots to facilitate imaging.

1.3 In vitro MSC proliferation on the 3D printed osteochondral scaffolds

Primary human bone marrow MSCs were derived from healthy consenting donors from the Texas A&M Health Science Center and thoroughly characterized. It will be used to evaluate the cytocompatibility properties of the 3D printed scaffolds. MSCs (passage #3-6) was cultured in a standard MSC growth media comprised of Alpha Minimum Essential medium supplemented with 16.5% fetal bovine serum, 1% (v/v) L-Glutamine, and 1% penicillin:streptomycin solution and cultured under standard cell culture conditions (37°C, a humidified, 5% CO2/95% air environment). They were subsequently lifted from cell culture flasks using Trypsin-EDTA for in vitro proliferation study.

A five day proliferation study was conducted on six osteochondral scaffolds and one collagen coated bi-phasic key scaffold in 24 well plates, with cells seeded at 100,000 cells per scaffold and 2 mL of media per well. Media was changed every other day, and cells were lifted for analysis at 1, 3 and 5 days. Thermoscientific photometric cell counting reagent (MTS assay) was used to quantify cell proliferation numbers and the result was read using a Thermo Scientific Multiskan GO microplate reader at a setting of 490 nm wavelength light.

1.4 In vitro MSC chondrogenic differentiation on the 3D printed osteochondral scaffolds

A two week differentiation study was also conducted on scaffolds with optimal pore density decided by MSC proliferation (i.e., small pore features). New scaffolds were fabricated, of the same physical specifications with small pores (control, bi-phasic, bi-phasic key scaffolds and bi-phasic key scaffold coated with collagen). MSCs were seeded at 150,000 cells per scaffold and cultured in the chondrogenic media including the MSC growth media with the addition of 100nM dexamethasone, 40 µg/ml proline, 100 µg/mL sodium pyruvate, 50 µg/mL L-Ascorbic acid 2-phosphate and 1% ITS+. Samples were then taken at 1 and 2 weeks and digested in a papain based enzymatic digestion solution for 24 hours at 60 ºC. Aliquots for appropriate assays were then taken from the bulk solutions. Glycosaminoglycan, Colalgen type II and total protein synthesis standard chondrogenic biochemistry assays were used to evaluate MSC chondrogenic differentiation in our 3D printed scaffolds.

2 RESULTS

2.1 Structure and mechanical characterization of 3D printed osteochondral scaffolds

Figure 1 show our novel cylindrical osteochondral construct design and printed scaffolds, with different internal structure. These homogenous and bi-

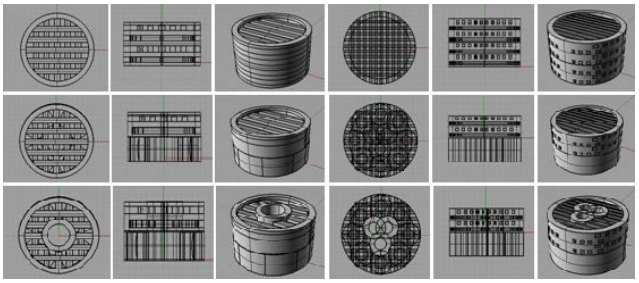

Figure 1; 3D designs of control, bi-phasic and key scaffolds

phasic scaffolds were designed to establish both a control group and a more traditionally designed osteochondral scaffold for comparison of key featured design. The homogenous model is a uniformly patterned structure, mimicking only one type of tissue. The bi-phasic scaffold is more similar to traditional osteochondral scaffolds [[3, 4]], containing both a cartilage and bone layer and no other materials or features. This key feature was designed to traverse the entire length of the scaffold, and penetrates both the cartilage and bone layer. It was intended to increase overall mechanical strength and to prevent failure of the device at the bi-phasic interface between the bone and cartilage layers. Physical characteristic data of all of printed scaffolds was computed from 3D models of all the scaffold groups. The total surface area of the construct increases from a homogenous design to a bi-phasic design, and again when a key feature is added. Furthermore, the total surface area of the construct increases again when the feature size is decreased from large to small pores. However, the surface area to volume ratio of the construct follows the opposite trend as described above. This is due to the fact that, with a decrease in feature size, more features can be added to the construct, thus increasing the overall volume, and is not a reflection of the surface to volume ratio of a given feature.

Mechanical compression tests were also conducted on the six different scaffold construct designs. All of the scaffolds showed excellent mechanical properties similar to or exceeding cartilage (0.75 to 1 MPa) and subchondral bone (30 to 50 Mpa) [[5-10]] in human osteochondral tissue. Under compressive loading, the bi-phasic key models both in small and large feature have the highest modulus when

compared to the homogeneous controls and the bi-phasic models. The bi-phasic scaffolds with large features performed better than the similar constructs with small features. Shear fracture energy testing was conducted on our bi-phasic key scaffold, bi-phasic scaffold and homogeneous controls, with three varying pore sizes, for a total of nine scaffolds. In all cases, the scaffolds showed a trend in the force per unit area that it took to cleave the scaffolds apart, increasing from the homogeneous control to

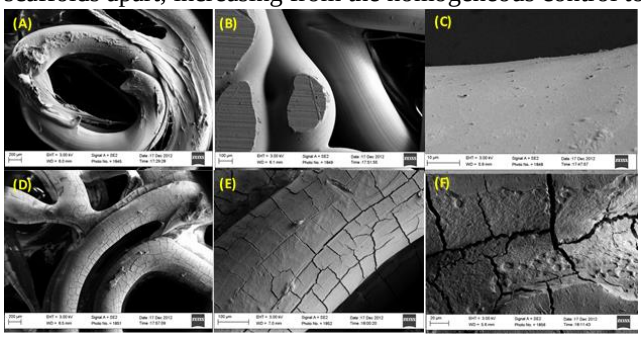

the bi-phasic model to our novel key model. Moreover, the surface morphology of our collagen modified scaffolds was imaged by SEM as shown in Figure 2. These scaffolds exhibited a collagen nono-texturing when compared to unmodified controls.

Figure 2; SEM images of (A-C) uncoated and (D-F) acetylated collagen type I coated 3D printed osteochondral scaffolds.

2.2 Improved MSC proliferation and chondrogenic differentiation in vitro

For two week chondrogenic differentiation, each sample was analyzed for GAG, total protein and collagen type II synthesis. Results of the GAG assay showed that the most GAG deposition was present on the key and collagen coated key scaffolds after one and two weeks. More interestingly, all samples showed an increase, with the far greatest increase on the key scaffold, except on the collagen coated key scaffold.

In contrast to our GAG result, all bi-phasic and bi-phasic key scaffolds with and without collagen coating showed greatly enhanced type II collagen deposition when compared to controls. All samples showed increased type II collagen synthesis when compared to week one. Increased total protein content was observed on bi-phasic, key scaffold with/without collagen coating after one week when compared to controls, with the most total protein present on the key model. At week two all samples continued to increase when compared to controls, but with the largest increase on the collagen type I coated scaffolds.

3 Discussion

Traditional approaches to osteochondral scaffold engineering often fail at the interface [[11, 12]], necessitating a construct with robust integration between cartilage and bone [[13-15]]. Our shear fracture results demonstrate that in addition to providing an advanced 3D fabrication technique that yields a scaffold with complex internal structure, 3D printing has the ability to achieve pre-designed structures which may provide a scaffold with better interfacial integration. The mechanical compression results also demonstrated that the inclusion of the key feature can greatly increase the compressive young's modulus when compared to other control. As we decreased the pore size of our constructs, we were able to increase the number of pores in the scaffold, and thus increase the overall porosity.The large pore scaffolds showed slightly higher moduli than small pore scaffolds. This may be due to the fact that, as the porosity of a material increases, its overall compressive modulus decreases [[16, 17]]. This increase in bulk porosity of the small featured scaffolds may be responsible for the decrease in mechanical performance.

Our MSC proliferation results demonstrated that both small pore feature and acetylated collagen modification can greatly promote MSC growth. Research has already shown that 3D printed constructs can be easily enhanced with bioactive coatings post-fabrication, for improved cell functions. For instance, Poldervaart et al. 3D printed bone constructs containing gelatin encapsulated BMP-2 [[18]]. They further enhanced the scaffolds with a calcium phosphate coating. The scaffold showed promising results when seeded with goat multipotent stromal cells. Cells displayed enhanced osteogenic activity after three weeks, and bone formation was observed after an in vivo study where constructs were subcutaneously implanted in rats and mice. While these results are promising, the effects and use of more exotic modification has not been extensively explored for 3D printed osteochondral constructs. The collagen surface modification method used in our study can be used to improve the cytocompatibility properties of 3D printed osteochondral construct and has the potential for use as suitable substrates on bulk scaffold structures for conjugating various bioactive factors (such as peptide and growth factors) with 3D printed scaffolds.

Our key feature scaffolds exhibited excellent performance in improving chondrogenic differentiation of MSCs in vitro when compared to controls. This is likely due to the face that the key scaffolds have greater surface area, while maintaining a comparable surface area to volume ratio to the bi-phasic model (Table I). Our collagen coating further enhanced cartilage protein deposition for some materials but not others. This was not wholly expected, but can be explained. GAG deposition is especially sensitive to culture surroundings. It is possible that scaffolds coated with collagen type I may have actually interfered with chondrogenic potential of cultured MSCs, or at the very least with their GAG synthesis and deposition. It has been well established that specific chemical factors can attribute to differential fates of MSCs [[19-21]]. Furthermore, production of specific ECM components of differentiated or partially differentiated stem cells can gain dominance over

the fate of the cellular community, and suppresses other protein / material production [[20, 22]]. Farrell et al. conducted an osteogenic study with MSCs cultured in 2D and 3D on novel collagen-GAG composite scaffolds [[23]]. They showed that, when cultured in osteogenic media, scaffolds with incorporated GAG expressed a higher amount of GAG deposition. Work in the field of MSC differentiation suggests that tissue specific materials, when present in a scaffold, elicit the formation of those materials and others specific to the tissue ECM they reside therein. We believe that this is why, when subjected to chondrogenic differentiation, collagen type I scaffolds underperformed in GAG material deposition. Collagen type I is the key collagen species present in subchondral bone ECM, hence its original selection. It was originally incorporated into our osteochondral scaffolds to add a biomimetic nanotextured coating, and to demonstrate the ease and ability to modify 3D printed scaffolds post-fabrication. There are, however, many other bioactive materials, natural polymers and nanobiomaterials that could be implemented (i.e. GAG and collagen type II for the cartilage layer, nHA for the bone layer, TGF-β1 or BMP-2 loaded nanospheres / functionalized nanotubes, etc.). Future iterations of our scaffolds could easily incorporate other coatings, and even have localized coatings for spatiotemporal osteochondral differentiation (e.g. collagen type I coating the bone layer and collagen type II coating the cartilage layer).

REFERENCES

1. Shipley, R.J., et al., *Design criteria for a printed tissue engineering construct: a mathematical homogenization approach.* J Theor Biol, 2009. **259**(3): p. 489-502.
2. Aishwarya, S., S. Mahalakshmi, and P.K. Sehgal, *Collagen-coated polycaprolactone microparticles as a controlled drug delivery system.* J Microencapsul, 2008. **25**(5): p. 298-306.
3. Oliveira, J.M., et al., *Novel hydroxyapatite/chitosan bilayered scaffold for osteochondral tissue-engineering applications: Scaffold design and its performance when seeded with goat bone marrow stromal cells.* Biomaterials, 2006. **27**(36): p. 6123-37.
4. Jiang, C.C., et al., *Repair of porcine articular cartilage defect with a biphasic osteochondral composite.* J Orthop Res, 2007. **25**(10): p. 1277-90.
5. Hutmacher, D.W., *Scaffolds in tissue engineering bone and cartilage.* Biomaterials, 2000. **21**(24): p. 2529-43.
6. Slivka, M.A., C.C. Chu, and I.A. Adisaputro, *Fiber-matrix interface studies on bioabsorbable composite materials for internal fixation of bone fractures. I. Raw material evaluation and measurement of fiber-matrix interfacial adhesion.* J Biomed Mater Res, 1997. **36**(4): p. 469-77.
7. Schaefer, D., et al., *Tissue-engineered composites for the repair of large osteochondral defects.* Arthritis Rheum, 2002. **46**(9): p. 2524-34.
8. Newitt, D.C., et al., *In vivo assessment of architecture and micro-finite element analysis derived indices of mechanical properties of trabecular bone in the radius.* Osteoporos Int, 2002. **13**(1): p. 6-17.
9. Lima, E.G., et al., *The effect of applied compressive loading on tissue-engineered cartilage constructs cultured with TGF-beta3.* Conf Proc IEEE Eng Med Biol Soc, 2006. **1**: p. 779-82.
10. Kelly, D.J. and P.J. Prendergast, *Prediction of the optimal mechanical properties for a scaffold used in osteochondral defect repair.* Tissue Eng, 2006. **12**(9): p. 2509-19.
11. Broom, N.D., et al., *Dynamic fracture characteristics of the osteochondral junction undergoing shear deformation.* Med Eng Phys, 1996. **18**(5): p. 396-404.
12. Flachsmann, E.R., N.D. Broom, and A. Oloyede, *A biomechanical investigation of unconstrained shear failure of the osteochondral region under impact loading.* Clin Biomech (Bristol, Avon), 1995. **10**(3): p. 156-165.
13. Silyn-Roberts, H. and N.D. Broom, *Fracture behaviour of cartilage-on-bone in response to repeated impact loading.* Connect Tissue Res, 1990. **24**(2): p. 143-56.
14. Kumar, P., et al., *Mechanical strength of osteochondral junction.* Nihon Seikeigeka Gakkai Zasshi, 1991. **65**(11): p. 1070-7.
15. Hayes, D.W., Jr., R.L. Brower, and K.J. John, *Articular cartilage. Anatomy, injury, and repair.* Clin Podiatr Med Surg, 2001. **18**(1): p. 35-53.
16. Hunger, P.M., A.E. Donius, and U.G. Wegst, *Structure-property-processing correlations in freeze-cast composite scaffolds.* Acta Biomater, 2013. **9**(5): p. 6338-48.
17. Nakai, M., M. Niinomi, and D. Ishii, *Mechanical and biodegradable properties of porous titanium filled with poly-L-lactic acid by modified in situ polymerization technique.* J Mech Behav Biomed Mater, 2011. **4**(7): p. 1206-18.
18. Poldervaart, M.T., et al., *Sustained Release of BMP-2 in Bioprinted Alginate for Osteogenicity in Mice and Rats.* PLoS ONE, 2013. **8**(8): p. e72610.
19. Jager, M., et al., *Proliferation and osteogenic differentiation of mesenchymal stem cells cultured onto three different polymers in vitro.* Ann Biomed Eng, 2005. **33**(10): p. 1319-32.
20. Curran, J.M., R. Chen, and J.A. Hunt, *Controlling the phenotype and function of mesenchymal stem cells in vitro by adhesion to silane-modified clean*

glass surfaces. Biomaterials, 2005. **26**(34): p. 7057-67.
21. Li, W.J., et al., *Multilineage differentiation of human mesenchymal stem cells in a three-dimensional nanofibrous scaffold.* Biomaterials, 2005. **26**(25): p. 5158-66.
22. Ishii, M., et al., *Molecular markers distinguish bone marrow mesenchymal stem cells from fibroblasts.* Biochem Biophys Res Commun, 2005. **332**(1): p. 297-303.
23. Farrell, E., et al., *A comparison of the osteogenic potential of adult rat mesenchymal stem cells cultured in 2-D and on 3-D collagen glycosaminoglycan scaffolds.* Technol Health Care, 2007. **15**(1): p. 19-31.
24. Matsubara, T., et al., *A new technique to expand human mesenchymal stem cells using basement membrane extracellular matrix.* Biochem Biophys Res Commun, 2004. **313**(3): p. 503-8.